Coupled-mode analysis of contra-directional coupling between two asymmetric photonic crystal waveguides

Vakhtang Jandieri,[1,*] Kiyotoshi Yasumoto,[2] and Jaromir Pistora[3]

[1]*Aghmashenebeli Alley 140, Department of Computer and Electrical Engineering, Free University of Tbilisi, 0159 Tbilisi, Georgia*
[2]*College of Information Science and Technology, Nanjing Forestry University, Nanjing 210037, China*
[3]*Nanotechnology Centre, VSB-Technical University of Ostrava 17. listopadu 15, 708 33 Ostrava-Poruba, Czech Republic*
**Corresponding author: jandieri@ee.knu.ac.kr*

Received November 25, 2013; accepted December 21, 2013;
posted January 6, 2014 (Doc. ID 201755); published February 13, 2014

A self-contained coupled-mode theory for the coupled two asymmetric photonic crystal waveguides (PCWs) is presented. The first-order coupled-mode equations are derived under a weak coupling assumption. The coupling coefficients are obtained systematically by a matrix calculus using the modal solutions of each PCW in isolation. The coupled-mode equations are solved for contra-directional coupling between two asymmetric PCWs formed by a hexagonal lattice of circular air holes in a dielectric medium. The power transmission spectra at different output ports of the coupled PCWs are investigated. It is shown that the self-contained coupled-mode analysis is useful to characterize a peculiar feature of the contra-directionally coupled PCWs as a drop filter.

OCIS codes: (050.5298) Photonic crystals; (130.2790) Guided waves; (130.5296) Photonic crystal waveguides.
http://dx.doi.org/10.1364/JOSAA.31.000518

1. INTRODUCTION

Photonic crystals (PCs) have inspired a lot of interest due to their wide application for controlling the propagation of light [1,2]. A photonic crystal waveguide (PCW) is made by removing a row of either air columns or dielectric rods that result in multimode guiding [3,4]. If the PCWs are placed in close proximity, a coupled PCW is formed, and the optical power is efficiently transferred from one PCW to another. Recently, coupled PCWs have received much attention due to their promising applications to ultra-compact, miniaturized photonic devices, such as filters, switches, power dividers, and couplers.

The optical propagation in the coupled PCWs has been extensively analyzed using the plane wave expansion method [5–8], the finitedifference time-domain method [5,7–11], the scattering matrix method combined with the lattice sums technique [12,13], and the coupled-mode theory [5,6,9,10]. Among others, the coupled-mode theory is an analytical method based on a perturbation theory and gives an approximate solution, which enables us to get a clear picture on the power transfer between two PCWs. The coupled-mode theory has been successfully used to model guided-wave devices based on the conventional optical waveguides, in which the coupling coefficients have been calculated in self-contained way [14,15] using a perturbation analysis or an overlap integral between the mode fields of uncoupled waveguides. However, the previous pertinent studies on the coupled-mode theory of PCWs have mostly assumed a prescribed form of the coupled-mode equations and calculated the coupling coefficients by using the propagation constants of supermodes supported in the coupled PCWs that were obtained by other numerical methods.

Recently, the present authors have proposed a self-contained coupled-mode formulation [16] for two parallel-coupled PCWs and derived systematically the coupled-mode equations by using the first-order perturbation theory for a weak coupling. In this formulation, the coupling coefficients are obtained by a matrix calculus based on the eigenmode solutions in each individual PCW in isolation. The coupled-mode equations have been used [16] to analyze a codirectional coupling between two symmetric PCWs with square lattice of circular rods in a free space or circular air holes in a dielectric medium.

In this paper, we shall apply the proposed coupled-mode formulation to a contra-directional coupling between two asymmetric PCWs. In Section 2, we briefly explain the calculation procedure to obtain the coupled-mode equations for two coupled PCWs, which govern the evolution of the modal amplitudes in individual PCWs. The formal solutions of the coupled-mode equations are also discussed. The contra-directional coupling between two PCWs with hexagonal lattice of circular air holes in a dielectric medium [9] is numerically studied in Section 3. When the modes of two single isolated PCWs interact at the phase-matching point, the repulsion effect between the guided modes appears, and the contra-directional coupling between the forward and backward waves occurs. The dispersion diagrams of the isolated PCWs as well as the dispersion curves of the coupled two asymmetric PCWs are studied. The optical power exchange between two PCWs is investigated, and the output powers at different ports of the contra-directional PCWs coupler are analyzed. It is shown that about 80% of the initial power is transferred

contra-directionally from one PCW to another. A conclusion is given in Section 4.

2. COUPLED MODE FORMULATION FOR TWO PHOTONIC CRYSTAL WAVEGUIDES

The schematic view of a coupled 2D PCW structure is shown in Fig. 1(a). The guiding layers a and b with widths, w_a and w_b, which are bounded by the upper and lower PCs, respectively, are separated by the intermediate barrier layer of a PC. We do not specify here the particular configuration of three PC layers except that they are formed by parallel circular rods, which are infinitely long in the y direction and have a common lattice constant h in the z direction. There exist TE and TM modes in the 2D PCWs. We consider here the TE mode having the electric and magnetic field components (E_y, H_x, H_z). The TM mode having the field components (H_y, E_x, E_z) can be treated in the same way.

In the first-order coupled-mode analysis, the guided field supported by the two-parallel waveguide system is approximated as follows:

$$\psi(x,z) = A(z)\sum_{m=-\infty}^{\infty}\alpha_a c_{a,m}p_{a,m}(x)\exp(i\beta_{a,m}z) + B(z)\sum_{m=-\infty}^{\infty}\alpha_b c_{b,m}p_{b,m}(x)\exp(i\beta_{b,m}z), \quad (1)$$

where $\beta_{a,m} = \beta_a + 2m\pi/h$, $\beta_{b,m} = \beta_b + 2m\pi/h$, β_a, and β_b are the propagation constants of the mode field supported by each single PCW a and b in isolation as shown in Figs. 1(b) and 1(c), $p_{a,m}(x)$ and $p_{b,m}(x)$ denote the transverse field distribution functions of the mth order Floquet modes in two isolated PCWs, $c_{a,m}$ and $c_{b,m}$ are the amplitudes of the Floquet mode, $A(z)$ and $B(z)$ denote the slowly varying amplitudes, which characterize the coupling between two PCWs. If the configuration of the PCW system is specified, β_j, $c_{j,m}$, and $p_{j,m}(x)$ $(j = a, b)$ can be calculated [12,13] by using the lattice sums and scattering matrix of layered periodic arrays of circular rods. In Eq. (1), α_a and α_b are the normalization constants introduced so that the power carried by each waveguide mode per unit length in the y direction satisfies the relations:

$$\frac{1}{2\omega\mu_0}\sum_{m=-\infty}^{\infty}\alpha_j^2\beta_{j,m}|c_{j,m}|^2\int_{-\infty}^{\infty}|p_{j,m}(x)|^2\mathrm{d}x = \pm 1 \qquad (j = a, b), \quad (2)$$

where the plus (minus) sign in Eq. (2) corresponds to the forward (backward) propagating modes. Using the first-order perturbation analysis to Eq. (1), the coupled-mode equations for the coupled PCWs are obtained as follows [16]:

$$\frac{d}{dz}A(z) = i\exp(-i\Delta\beta z)\kappa_{ab}B(z), \quad (3)$$

$$\frac{d}{dz}B(z) = i\exp(i\Delta\beta z)\kappa_{ba}A(z), \quad (4)$$

with

$$\kappa_{ab} = \frac{\alpha_b \boldsymbol{g}_a^T\cdot\mathbf{D}_{ab}(\omega,\beta_b)\cdot\boldsymbol{c}_b}{\alpha_a \boldsymbol{g}_a^T\cdot\frac{\partial\mathbf{D}_a(\omega,\beta_a)}{\partial\beta_a}\cdot\boldsymbol{c}_a}, \quad (5)$$

$$\kappa_{ba} = \frac{\alpha_a \boldsymbol{g}_b^T\cdot\mathbf{D}_{ba}(\omega,\beta_a)\cdot\boldsymbol{c}_a}{\alpha_b \boldsymbol{g}_b^T\cdot\frac{\partial\mathbf{D}_b(\omega,\beta_b)}{\partial\beta_b}\cdot\boldsymbol{c}_b}, \quad (6)$$

$$\mathbf{D}_a(\omega,\beta) = \mathbf{I} - \mathbf{W}_a(\omega,\beta)\bar{\bar{\mathbf{R}}}_U^{N_U}(\omega,\beta)\mathbf{W}_a(\omega,\beta)\bar{\bar{\mathbf{R}}}_B^{N_\infty}(\omega,\beta), \quad (7)$$

$$\mathbf{D}_b(\omega,\beta) = \mathbf{I} - \mathbf{W}_b(\omega,\beta)\bar{\bar{\mathbf{R}}}_L^{N_L}(\omega,\beta)\mathbf{W}_b(\omega,\beta)\bar{\bar{\mathbf{R}}}_B^{N_\infty}(\omega,\beta), \quad (8)$$

$$\mathbf{D}_{ab}(\omega,\beta) = \mathbf{W}_a(\omega,\beta)\bar{\bar{\mathbf{R}}}_U^{N_U}(\omega,\beta)\mathbf{W}_a(\omega,\beta)\bar{\bar{\mathbf{T}}}_B^{N_B}(\omega,\beta), \quad (9)$$

$$\mathbf{D}_{ba}(\omega,\beta) = \mathbf{W}_b(\omega,\beta)\bar{\bar{\mathbf{R}}}_L^{N_L}(\omega,\beta)\mathbf{W}_b(\omega,\beta)\bar{\bar{\mathbf{T}}}_B^{N_B}(\omega,\beta), \quad (10)$$

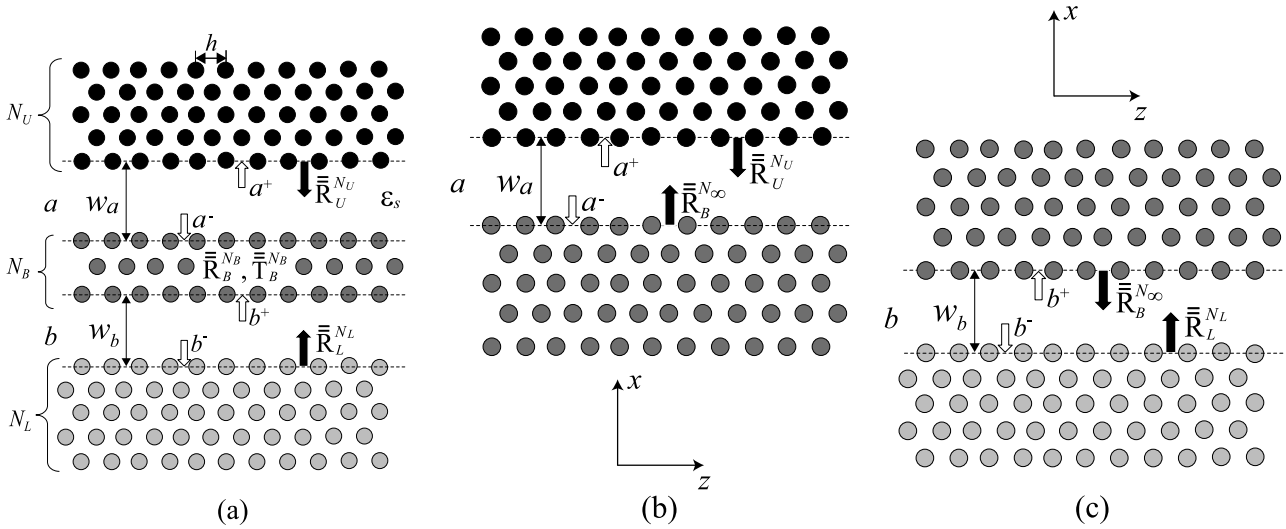

Fig. 1. Schematics of the coupled parallel PCWs: (a) coupled PCW system, (b) isolated PCW a, and (c) isolated PCW b. The circular rods forming the PCW are parallel and infinitely long in the y direction. The waveguide problem is 2D.

$$\mathbf{W}_a(\omega,\beta)=[\exp(i\gamma_{a,m}w_a)\delta_{mn}],\mathbf{W}_b(\omega,\beta)=[\exp(i\gamma_{b,m}w_b)\delta_{mn}], \tag{11}$$

where $k_s=\omega\sqrt{\varepsilon_s\mu_0}$, $\gamma_{a,m}=\sqrt{k_s^2-\beta_{a,m}^2}$, $\Delta\beta=\beta_a-\beta_b$, $\gamma_{b,m}=\sqrt{k_s^2-\beta_{b,m}^2}$, and $\boldsymbol{g}_a$ and $\boldsymbol{g}_b$ are the right eigenvectors that satisfy relations $\mathbf{D}_a^T(\omega,\beta_a)\cdot\boldsymbol{g}_a=\mathbf{0}$ and $\mathbf{D}_b^T(\omega,\beta_b)\cdot\boldsymbol{g}_b=\mathbf{0}$, and the superscript T denotes the transpose of the indicated vectors and matrices. In Eqs. (7) to (10), $\bar{\bar{\mathbf{R}}}_\nu^{N_\nu}(\omega,\beta)$ $(\nu=U,L)$ are the generalized reflection matrices of the upper and lower PC structures viewed from the guiding layers a and b, $\bar{\bar{\mathbf{T}}}_B^{N_B}(\omega,\beta)$ is the generalized transmission matrix of the N_B layered PC barrier, and $\bar{\bar{\mathbf{R}}}_B^{N_\infty}(\omega,\beta)$ is the generalized reflection matrix of the PC barrier structure with an enough layers, N_∞, so that the two guiding layers, a and b, are well separated.

When the lattice constants, the material parameters of circular rods and the background medium, and the numbers of layers (N_U,N_B,N_∞,N_L) are specified, $\bar{\bar{\mathbf{R}}}_\nu^{N_\nu}(\omega,\beta)$ $(\nu=U,L)$, $\bar{\bar{\mathbf{T}}}_B^{N_B}(\omega,\beta)$, and $\bar{\bar{\mathbf{R}}}_B^{N_\infty}(\omega,\beta)$ are accurately calculated by the standard matrix calculus using the lattice sums, the T-matrix of circular rods, and the scattering matrix of a periodic array of circular rods [16,17].

The general solution to Eqs. (3) and (4) for the mode amplitudes $A(z)$ and $B(z)$ are obtained in the following form:

$$A(z)=A_1\exp(i\eta_{a,1}z)+A_2\exp(i\eta_{a,2}z), \tag{12}$$

$$B(z)=A_1\frac{\kappa_{ba}}{\eta_{b,1}}\exp(i\eta_{b,1}z)+A_2\frac{\kappa_{ba}}{\eta_{b,2}}\exp(i\eta_{b,2}z), \tag{13}$$

with

$$\eta_{a,1}=-\frac{\Delta\beta}{2}+\frac{q}{2},\qquad \eta_{a,2}=-\frac{\Delta\beta}{2}-\frac{q}{2}, \tag{14}$$

$$\eta_{b,1}=\frac{\Delta\beta}{2}+\frac{q}{2},\qquad \eta_{b,2}=\frac{\Delta\beta}{2}-\frac{q}{2}, \tag{15}$$

$$q=\sqrt{(\Delta\beta)^2+4\kappa_{ab}\kappa_{ba}}, \tag{16}$$

where A_1 and A_2 are the unknown constants, which are determined using the initial excitation conditions. Equations (14) and (15) give the perturbations to the propagation constants $\beta_a(\omega)$ and $\beta_b(\omega)$ of two isolated PCWs a and b as functions of ω.

Due to the coupling between two PCWs, each of original propagation constants, $\beta_a(\omega)$ and $\beta_b(\omega)$, are split into two propagation constants in the neighborhood of the phase-matching point, which satisfies $\omega=\omega_0$ and $\beta_a(\omega_0)=\beta_b(\omega_0)$ as follows:

$$\beta_{1,2}(\omega)=\beta_a(\omega)-\frac{\Delta\beta(\omega)}{2}\pm\frac{q(\omega)}{2}, \tag{17}$$

$$\beta_{3,4}(\omega)=\beta_b(\omega)+\frac{\Delta\beta(\omega)}{2}\pm\frac{q(\omega)}{2}, \tag{18}$$

where β_a, β_b, $\Delta\beta$, and q are specified as functions of frequency ω for understanding the phase-matching condition between two waveguide modes. For a contra-directional coupling, we assume that the wave with the unit amplitude is initially excited at the right end $z=l$ of the upper waveguide a. In the lower waveguide b, the wave travels in the direction opposite to waveguide a, and there is no initial excitation at the left end of the coupler at $z=0$. This leads to the following initial conditions:

$$A(z=l)=1,\qquad B(z=0)=0. \tag{19}$$

With the initial condition in Eq. (19) together with Eqs. (12) and (13), the modal amplitudes of the coupled mode equations are expressed in the following form:

$$A(z)=\frac{q\cos\left(\frac{q}{2}z\right)+i\Delta\beta\sin\left(\frac{q}{2}z\right)}{q\cos\left(\frac{q}{2}l\right)+i\Delta\beta\sin\left(\frac{q}{2}l\right)}\exp\left[i\frac{\Delta\beta}{2}(l-z)\right], \tag{20}$$

$$B(z)=\frac{i2\kappa_{ba}\sin\left(\frac{q}{2}z\right)}{q\cos\left(\frac{q}{2}l\right)+i\Delta\beta\sin\left(\frac{q}{2}l\right)}\exp\left[i\frac{\Delta\beta}{2}(z+l)\right]. \tag{21}$$

3. NUMERICAL RESULTS AND DISCUSSION

The contra-directional coupling between two asymmetric PCWs consisting of the hexagonal lattice of circular air holes in a dielectric background medium is analyzed by using the proposed coupled-mode formulation. The PCW structure to be analyzed is the same as investigated in [9] by using the FDTD method. We assume that the permittivity of the background medium is $\varepsilon_s=10.5\varepsilon_0$ and the radius of the air holes is $r=0.36h$. The width of the upper PCW is $w_a=0.8\sqrt{3}h$, and the width of the lower PCW is $w_b=\sqrt{3}h$. The air-hole-type PC has a photonic bandgap for the E polarized field (E_y,H_x,H_z). The initial excitation is launched into the upper PCW at $z=l$.

First we discuss the dispersion diagram of the coupled asymmetric PCWs with a one-layer barrier, $(N_B=1)$, structure as shown in Fig. 2. The mode propagation constants, $\beta_a(\omega)$ and $\beta_b(\omega)$, for each isolated single PCW a and b were calculated as functions ω by using the semi-analytical method presented in [13]. The dispersion diagrams for two isolated PCWs calculated by assuming $N_U=N_L=N_\infty=10$ are shown in Figs. 3 and 4. From these two figures, we can see that the upper PCW with $w_a=0.8\sqrt{3}h$ supports three guided modes, whereas the lower PCW with $w_b=\sqrt{3}h$ supports four guided modes.

When the two PCWs are placed in close proximity, the mode fields in each isolated PCW interact in the neighborhood of the phase-matching point, which satisfies $\omega=\omega_0$ and $\beta_a(\omega_0)=\beta_b(\omega_0)$ in the dispersion diagrams. The interaction causes repulsion between two original dispersion curves, which intersect at the phase-matching point and create a new dispersion diagram for the contra-directional coupling between the forward and backward propagating modes. Using the numerical results shown in Figs. 3 and 4, the phase-matching point is calculated as $h/\lambda_0=0.3428$ and $\beta_a(\omega_0)h/2\pi=\beta_b(\omega_0)h/2\pi=0.0455$, where $\lambda_0=2\pi c_0/\omega_0$, and c_0 is the velocity of light in a free space. Figure 5(a) illustrates the dispersion diagrams for the coupled PCWs with $N_B=1$

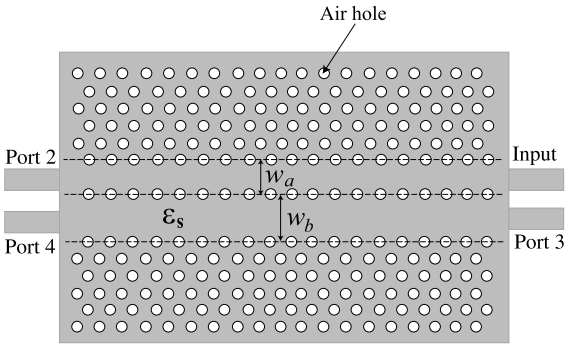

Fig. 2. Schematic view of a contra-directionally coupled two asymmetric PCWs consisting of the hexagonal lattice of circular air holes with radius $r = 0.36h$ being located in a background medium with $\varepsilon_s = 10.5\varepsilon_0$. The widths of guiding layers in the upper and lower PCWs are $w_a = 0.8\sqrt{3}h$ and $w_b = \sqrt{3}h$, respectively. The number of barrier layers between two PCWs is $N_B = 1$. The initial excitation is launched in the upper PCW at $z = l$.

calculated by the rigorous analysis based on the lattice sums technique combined with the T-matrix approach [13,17]. It is seen that the guided modes are perturbed in the whole frequency range due to the strong coupling between two asymmetric PCWs.

The region where the contra-directional coupling occurs is surrounded by a gray rectangle, and the enlarged diagram in the coupling region is plotted in Fig. 5(b) by the solid lines. The normalized propagation constant, $\beta(\omega)h/2\pi$, which is calculated using the coupled-mode analysis in Eqs. (17) and (18), is also plotted by the dashed line in Fig. 5(b). We can see that for a one-layer barrier structure, the propagation constants of the coupled waves calculated by the coupled-mode analysis are not in good agreement with those of the rigorous analysis. This is because the contra-directional coupling between two asymmetric PCWs through a one-layer barrier structure falls into a category of strong coupling, whereas the proposed coupled-mode analysis based on the perturbation theory assumes weak coupling. When the number of the barrier layers is increased, however, a situation of relatively weak coupling between two asymmetric PCWs is realized.

Next, we consider the contra-directional coupling of the same asymmetric PCWs but having a three-layered barrier

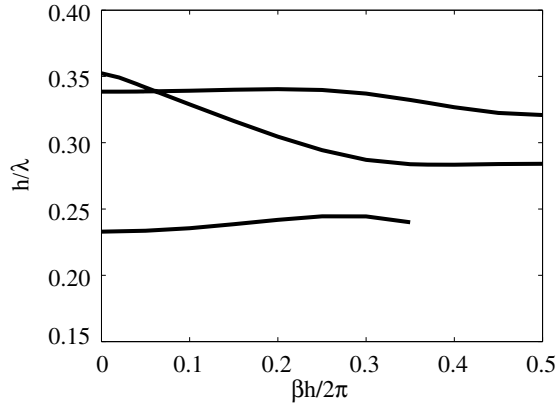

Fig. 3. Dispersion diagrams for the upper PCW "a" in isolation, which consists of the hexagonal lattice of circular air-holes with radius $r = 0.36h$ located in a background dielectric with $\varepsilon_s = 10.5\varepsilon_0$, where $w_a = 0.8\sqrt{3}h$ and $N_U = N_\infty = 10$.

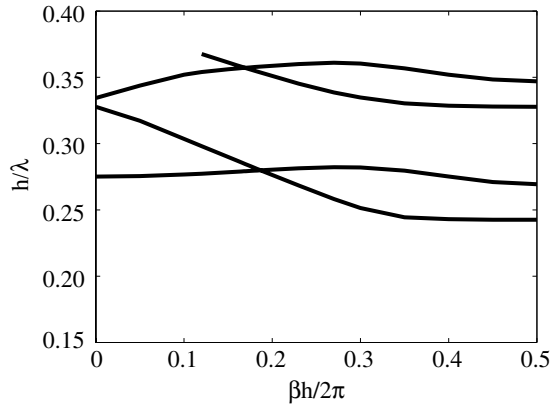

Fig. 4. Dispersion diagrams for the lower PCW b in isolation, which consists of the hexagonal lattice of circular air holes with radius $r = 0.36h$ located in a background dielectric with $\varepsilon_s = 10.5\varepsilon_0$, where $w_b = \sqrt{3}h$ and $N_L = N_\infty = 10$.

($N_B = 3$) structure as shown in Fig. 6. Figure 7(a) illustrates the dispersion curves of the coupled PCWs with a three-layered barrier structure calculated by rigorous analysis [13,17]. The region where the contra-directional coupling occurs is surrounded by the gray rectangle, and the enlarged dispersion diagram in the neighborhood of the phase-matching point is plotted in Fig. 7(b). We can see that the

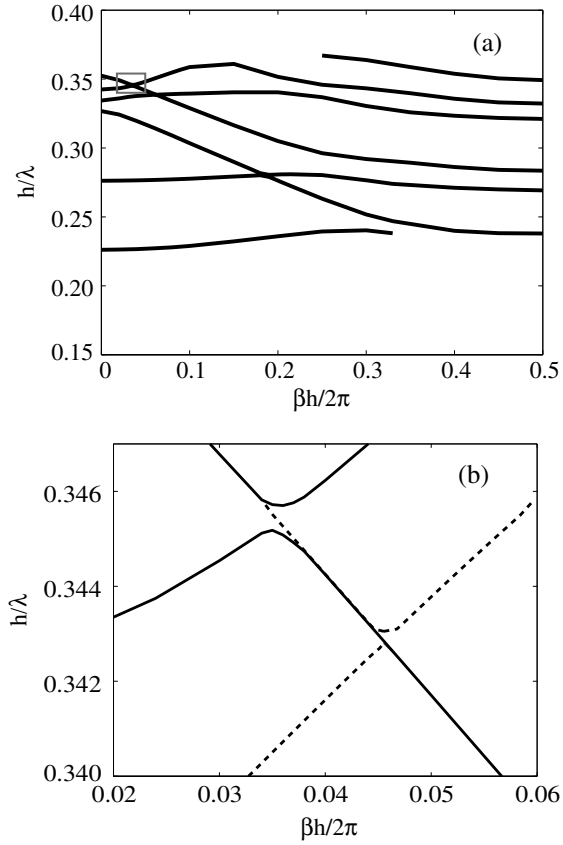

Fig. 5. (a) Dispersion diagrams of the guided modes for the coupled asymmetric PCWs as shown in Fig. 2, where the number of barrier layers between two PCWs is $N_B = 1$. (b) Enlarged dispersion diagrams for the coupling region surrounded by a gray rectangle in (a). The solid lines are obtained by the rigorous analysis [13], and the dashed lines present the results of the coupled-mode analysis given by Eqs. (17) and (18).

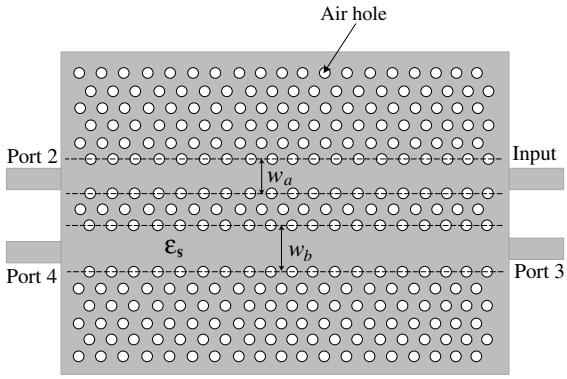

Fig. 6. The same as in Fig. 2, but for three-layered barrier structure with $N_B = 3$.

propagation constants (dashed line) of the coupled waves calculated by the coupled-mode analysis in Eqs. (17) and (18) are in close agreement with those of the rigorous analysis (solid line). Thus the proposed coupled-mode analysis can be used to analyze the contra-directional coupling between two asymmetric PCWs with a barrier structure of three layers or more. For the three-layered barrier structure, Eqs. (20) and (21) were calculated. Figure 8 shows the guided powers $|A(0)|^2$ in port 2 (solid line) and $|B(l)|^2$ in port 3 (dashed line) as functions of the normalized frequency h/λ, where the coupler

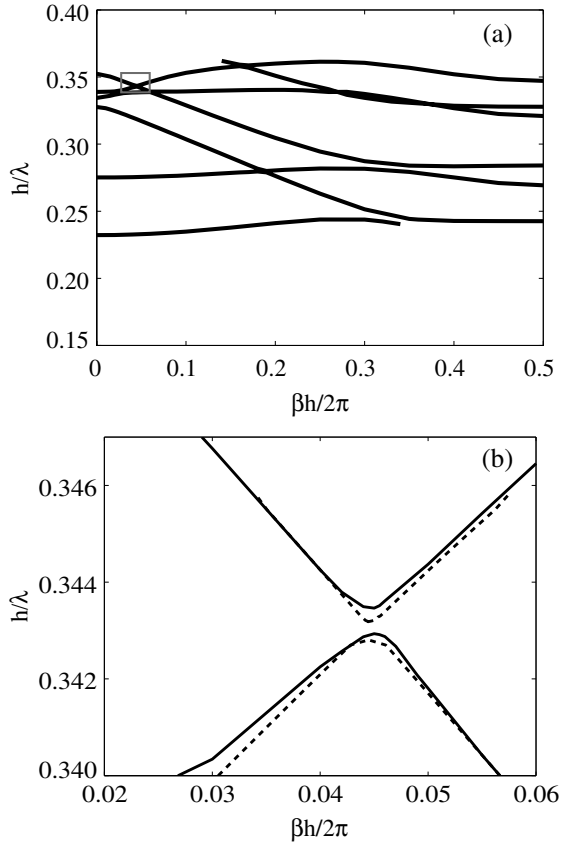

Fig. 7. (a) Dispersion diagrams of the guided mode for the coupled PCWs with $N_B = 3$ as shown in Fig. 6. (b) Enlarged dispersion diagrams for the coupling region surrounded by a gray rectangle in (a). The solid lines are obtained by rigorous analysis [13], and the dashed lines present the results of the coupled-mode analysis given by Eqs. (17) and (18).

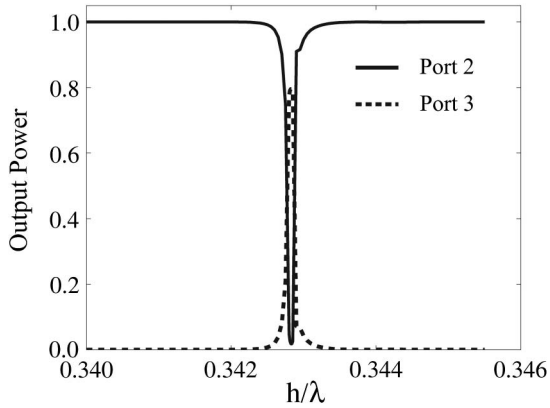

Fig. 8. Transmission power spectrum at different output ports calculated by the coupled-mode analysis in Eqs. (20) and (21) for the coupled PCWs with $N_B = 3$. The length of PCWs is $l = 2000h$, and the output port numbers correspond to those given in Fig. 6.

length is assumed to be $l = 2000h$. We can see that around 80% of the input power is dropped into the port 3 of the lower PCW at the resonant frequency $h/\lambda_0 = 0.3428$. The power transmission spectra in the same asymmetric PCWs coupler have been analyzed [9] for $N_B = 1$ and $l = 240h$ by using the finite-difference time-domain method. The peculiar feature of Fig. 8 agrees well with that (Fig. 4) of [9] except for the difference in the resonant frequency h/λ_0. In the coupled-mode analysis, the resonant frequency is given by the frequency of phase matching at which the dispersion curves of two PCWs in isolation intersect each other. When $N_B = 1$, coupling is strong, and the coupling region is shifted from the phase-matching frequency $h/\lambda_0 = 0.3428$ as shown in Fig. 5(b), whereas when $N_B = 3$, the phase-matching frequency is just located inside the coupling region as shown in Fig. 7(b).

4. CONCLUSION

We have presented the coupled-mode formulation for two parallel-coupled PCWs based on the perturbation analysis. The formulation has been used to analyze contra- directional coupling between two asymmetric PCWs consisting of the hexagonal lattice of the circular air holes in a dielectric background medium. The dispersion diagrams of the isolated PCWs as well as the coupled PCWs and the effect of the barrier layers between two PCWs on their coupling characteristics have been numerically studied. It is proven that the present coupled-mode formulation is applicable when the barrier PC is of three layers or more. The coupled-mode equations have been solved for the case of three-layered barrier structure, and the power transmission spectra at different output ports of the coupled PCWs have been calculated. It is also shown that the coupled PCWs with a three-layered barrier can be used as a drop filter with around 80% drop in efficiency.

ACKNOWLEDGMENTS

This work was partially supported by the Centre of Excellence IT4Innovations project, reg. no. CZ.1.05/1.1.00/02.0070.

REFERENCES

1. E. Yablonovitch, "Inhibited spontaneous emission in solid-state physics and electronics," Phys. Rev. Lett. **58**, 2059–2062 (1987).
2. S. John, "Strong localization of photons in certain disordered dielectric superlattices," Phys. Rev. Lett. **58**, 2486–2489 (1987).

3. A. Adibi, Y. Xu, R. Lee, A. Yariv, and A. Scherer, "Properties of the slab modes in photonic crystal optical waveguides," J. Lightwave Technol. **18**, 1554–1564 (2000).
4. M. Qiu, K. Azizi, A. Karlsson, M. Swillo, and B. Jaskorzynska, "Numerical studies of mode gaps and coupling efficiency for line-defect waveguides in two-dimensional photonic crystals," Phys. Rev. B **64**, 155113 (2001).
5. A. Sharkawy, S. Shi, J. Murakowski, and D. W. Prather, "Analysis and applications of photonic crystals coupled waveguide theory," Proc. SPIE **4655**, 356–367 (2002).
6. S. Olivier, H. Benisty, C. Weisbuch, C. J. M. Smith, T. F. Krauss, and R. Houdré, "Coupled-mode theory and propagation losses in photonic crystal waveguides," Opt. Express **11**, 1490–1496 (2003).
7. J. Zimmermann, M. Kamp, A. Forchel, and R. Marz, "Photonic crystal waveguide directional couplers as wavelength selective optical filters," Opt. Commun. **230**, 387–392 (2004).
8. Y. Tanaka, H. Nakamura, Y. Sugimoto, N. Ikeda, K. Asakawa, and K. Inoue, "Coupling properties in a 2-D photonic crystal slab directional coupler with a triangular lattice of air holes," IEEE J. Quantum Electron. **41**, 76–84 (2005).
9. M. Qiu and M. Swillo, "Contra-directional coupling between two-dimensional photonic crystal waveguides," Photon. Nanostr. Fundam. Appl. **1**, 23–30 (2003).
10. Z. Xu, J. Wang, Q. He, L. Cao, P. Su, and G. Jin, "Optical filter based on contra-directional waveguide coupling in a 2D photonic crystal with square lattice of dielectric rods," Opt. Express **13**, 5608–5613 (2005).
11. E. Engin, J. L. O'Brien, and M. J. Cryan, "Design and analysis of a gallium nitride-on-sapphire tunable photonic crystal directional coupler," J. Opt. Soc. Am. B **29**, 1157–1164 (2012).
12. C. M. de Sterke, L. C. Botten, A. A. Asatryan, T. P. White, and R. C. McPhedran, "Modes of coupled photonic crystal waveguides," Opt. Lett. **29**, 1384–1386 (2004).
13. K. Yasumoto, H. Jia, and K. Sun, "Rigorous modal analysis of two-dimensional photonic crystal waveguides," Radio Sci. **40**(6), RS6S02, 1–7 (2005).
14. A. W. Snyder and J. D. Love, *Optical Waveguide Theory* (Chapman and Hall, 1983).
15. W.-P. Huang, "Coupled-mode theory for optical waveguides: an overview," J. Opt. Soc. Am. A **11**, 963–983 (1994).
16. K. Yasumoto, V. Jandieri, and Y. Liu, "Coupled-mode formulation of two-parallel photonic-crystal waveguides," J. Opt. Soc. Am. A **30**, 96–101 (2013).
17. K. Yasumoto, H. Toyama, and T. Kushta, "Accurate analysis of two-dimensional electromagnetic scattering from multilayered periodic arrays of circular cylinders using lattice sums technique," IEEE Trans. Antennas Propag. **52**, 2603–2611 (2004).